

Spectroscopic Characterization of a Copper(III) Trisuperoxide Complex Bearing Both Side-On and End-On Ligands

Yu Gong, Guanjun Wang, and Mingfei Zhou*

Department of Chemistry, Shanghai Key Laboratory of Molecular Catalysts and Innovative Materials, Advanced Materials Laboratory, Fudan University, Shanghai 200433, China

Received: February 3, 2009

The copper atom reacts with dioxygen in solid argon to form a mononuclear copper dioxygen complex $\text{Cu}(\eta^2\text{-O}_2)(\eta^1\text{-O}_2)_2$ bearing both side-on and end-on bonded O_2 ligands. The complex is characterized as being a trisuperoxide species with the copper center in its unusual +3 oxidation state. The Cu(III) trisuperoxide complex loses an end-on bonded superoxo ligand in forming the copper bisdioxygen complex under infrared irradiation.

Introduction

Dioxygen activation on copper sites is an important subject in biochemical oxidation. The copper center in enzymes is able to bind O_2 , which can further oxidize organic substrates via some copper dioxygen intermediates.¹ Compared to the rich studies on dinuclear copper–dioxygen complexes,² fewer examples were reported on the mononuclear copper dioxygen intermediates, which are highly reactive species. They can readily undergo dimerization reaction to give the more stable dicopper– O_2 adducts. Therefore, most of the mononuclear copper dioxygen complexes are transient species that could only be characterized by spectroscopic means or by use of stopped-flow method.³ Limited examples stabilized by bulky ligands at low temperature were structurally characterized using X-ray crystallography.^{4–6}

Mononuclear copper oxides and dioxygen complexes that serve as simple models in understanding the copper and dioxygen interactions have been the subject of a number of experimental^{7–15} and theoretical studies.^{16–25} In the case of CuO_6 , two isomers with the $\text{OCuO}(\text{O}_2)_2$ and $\text{Cu}(\text{O}_2)_3$ geometries were proposed to coexist in the gas phase from anion photoelectron spectroscopic study.²⁶ However, both structures were theoretically predicted not to be the global minima on the potential energy surfaces of CuO_6 . A bisozonide structure was calculated as the ground state for the CuO_6 complex using spin-polarized generalized gradient approximation (GGA) method with plane-wave basis sets,²⁷ whereas density functional theory (DFT) calculations using Perdew–Burke–Ernzerhof (PBE) functional predicted a trisuperoxide complex (C_{2v}) as the most stable configuration of CuO_6 .²⁸ Herein, we provide a joint matrix isolation infrared spectroscopic and theoretical characterization on a mononuclear copper trisuperoxide complex in solid argon in which the three O_2 ligands are coordinated to the copper center in both the side-on and end-on fashions.

Experimental and Computational Methods

The experimental setup for pulsed laser evaporation and matrix isolation infrared spectroscopic investigation has been described in detail previously.²⁹ Briefly, the 1064 nm fundamental of a Nd:YAG laser (Continuum, Minilite II, 10 Hz repetition rate and 6 ns pulse width) was focused onto a rotating copper target through a hole in a CsI window cooled normally

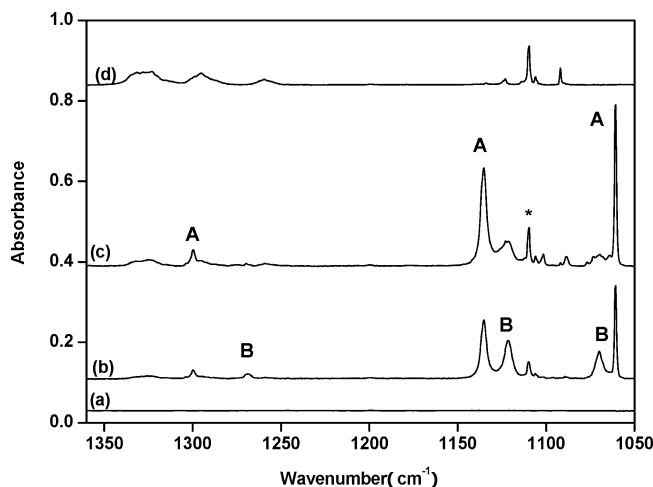


Figure 1. Infrared spectra in the 1360–1050 cm^{-1} region from co-deposition of laser-evaporated Cu atoms with 0.5% O_2 in argon. (a) 1 h of sample deposition at 6 K, (b) after annealing to 25 K with 10 scans, (c) after annealing to 35 K with 10 scans, and (d) after 10 min of $\lambda > 850$ nm irradiation. The asterisk denotes the absorption of the $\text{Cu}(\eta^2\text{-O}_2)_2$ complex.

to 6 K by means of a closed-cycle helium refrigerator (ARS, 202N). The laser-evaporated metal atoms were codeposited with dioxygen/argon mixtures onto the CsI window. In general, matrix samples were deposited for 1 h at a rate of approximately 4 mmol/h. The O_2/Ar mixtures were prepared in a stainless steel vacuum line using standard manometric technique. Isotopic $^{18}\text{O}_2$ (ISOTEC, 99%) was used without further purification. The infrared absorption spectra of the resulting samples were recorded on a Bruker IFS 66V spectrometer at 0.5 cm^{-1} resolution between 4000 and 450 cm^{-1} using a liquid nitrogen cooled HgCdTe (MCT) detector. Samples were annealed in the dark (out of the spectrometer beamline) to different temperatures and cooled back to 6 K for spectral acquisition, and selected samples were subjected to broadband irradiation using a tungsten lamp with glass filters. Typically, the infrared spectra were recorded with 150 scans but only 10 scans were employed in some cases due to the infrared-induced decrease of the product absorptions.

Quantum chemical calculations were performed using the Gaussian 03 program.³⁰ The three-parameter hybrid functional according to Becke with additional correlation corrections from

* To whom correspondence should be addressed. E-mail: mzhou@fudan.edu.cn.

TABLE 1: Infrared Absorptions (cm^{-1}) of the $\text{Cu}(\eta^2\text{-O}_2)(\eta^1\text{-O}_2)_2$ and $\text{Cu}(\eta^2\text{-O}_2)(\eta^1\text{-O}_2)_2(\text{O}_2)_x$ Complexes in Solid Argon

	$^{16}\text{O}_2$	$^{18}\text{O}_2$	$^{16}\text{O}_2+^{18}\text{O}_2$	$^{16}\text{O}_2+^{16}\text{O}^{18}\text{O}+^{18}\text{O}_2$	mode
$\text{Cu}(\eta^2\text{-O}_2)(\eta^1\text{-O}_2)_2$	1299.8	1227.2	1299.9, 1294.3, 1268.7, 1266.0, 1230.1, 1227.2	..., ^a 1282.3, 1266.6, 1263.7, 1247.0, ... ^a	$(\eta^1\text{-O}_2)_2$ sym.str.
	1135.2	1071.4	1135.3, 1097.4, 1071.4	1135.3, 1118.4, 1104.1, 1096.8, 1086.6, 1071.5	$(\eta^1\text{-O}_2)_2$ asym.str.
	1060.7	1000.9	1060.7, 1058.1, 1001.8	1059.7, 1058.2, 1031.0, 1001.9,	$\eta^2\text{-O}_2$ str.
$\text{Cu}(\eta^2\text{-O}_2)(\eta^1\text{-O}_2)_2(\text{O}_2)_x$	1269.0	1197.8			$(\eta^1\text{-O}_2)_2$ sym.str.
	1121.6	1058.8	1120.8, 1085.2, ... ^a		$(\eta^1\text{-O}_2)_2$ asym.str.
	1070.0	1009.1	..., ^a 1009.8	..., ^a 1039.6, 1009.8	$\eta^2\text{-O}_2$ str.

^a Absorptions unresolved because of weak intensities and band overlaps.

Lee, Yang, and Parr (B3LYP) was utilized.³¹ The 6-311+G(d) basis set was used for the O atom, and the all electron basis set of Wachters-Hay as modified by Gaussian was used for the Cu atom.³² The geometries were fully optimized, the harmonic vibrational frequencies were calculated, and zero-point vibrational energies were derived. The single-point energies of the structures optimized at the B3LYP level were calculated using the CCSD(T) method with the same basis set.

Results and Discussions

The reaction of laser-ablated copper atoms with dioxygen has been investigated previously.¹⁵ To favor the formation of oxygen-rich species and to prevent the production of multi-nuclear species, we employ relatively low evaporation laser energy. The infrared spectra in the O–O stretching region from co-deposition of laser-evaporated Cu atoms with 0.5% O_2 in argon are shown in Figure 1 with the product absorptions listed in Table 1. After 1 h of sample deposition, no product absorptions were observed in the spectrum except for a weak absorption at 953.7 cm^{-1} due to O_4^- anion (not shown in Figure 1).³³ When the as-deposited sample was annealed to 25 K, several sets of product absorptions were produced. The 1110.1 cm^{-1} absorption was observed in previous matrix isolation studies.^{7,8,15} In addition, six photosensitive absorptions were also observed, which can be divided into two groups (labeled as **A** and **B** in Figure 1) based on their behaviors upon sample annealing. The group **B** absorptions are broader than the group **A** ones. These absorptions decayed quickly with increasing sample scan times, indicating that the carriers for these bands are unstable toward infrared irradiation from the source of the spectrometer ($7500\text{--}370\text{ cm}^{-1}$). As shown in Figure 1 trace d, near-infrared irradiation using a tungsten lamp with a $\lambda > 850\text{ nm}$ long wavelength pass filter completely destroyed both group **A** and **B** absorptions. In concert, a broadband centered around 836.0 cm^{-1} increased at the expense of group **A** and **B** absorptions (shown in Figure 2). The 836.0 cm^{-1} absorption was previously suggested to the intraligand π^* electronic transition associated with coordinated dioxygen in $\text{Cu}(\text{O}_2)_2$, although the detailed structural information was not given.⁹ It should be pointed out that no copper oxide absorptions were observed in the present experiments. The 1110.1 cm^{-1} absorption was first observed in solid argon by Darling and co-workers who assigned it to the $\text{Cu}(\text{O}_2)_2$ complex with two equivalent O_2 fragments.⁷ The assignment was further confirmed by Tevault et al.⁸ However, in the latest matrix isolation study, this absorption was proposed to originate from a $(\text{CuOO})(\text{O}_2)_2$ complex.¹⁵ In the present experiments, no oxide species was observed; the spectroscopic characteristics are similar to those observed in the first two experiments. We suggest that the 1110.1 cm^{-1} absorption be due to the $\text{Cu}(\eta^2\text{-O}_2)_2$ complex.

Experiments were repeated under the same conditions using the $^{18}\text{O}_2$, $^{16}\text{O}_2+^{18}\text{O}_2$, and $^{16}\text{O}_2+^{16}\text{O}^{18}\text{O}+^{18}\text{O}_2$ samples to help

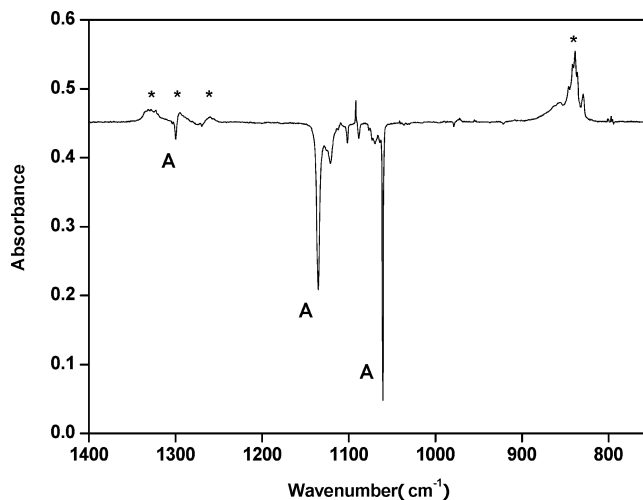


Figure 2. Difference IR spectra in the $1400\text{--}750\text{ cm}^{-1}$ region from co-deposition of laser-evaporated Cu atoms with 0.5% O_2 in argon. (Spectrum taken after 10 min of $\lambda > 850\text{ nm}$ irradiation minus spectrum taken after 35 K of sample annealing.) The asterisks denote the intraligand π^* electronic transition associated with coordinated dioxygen in $\text{Cu}(\text{O}_2)_2$.

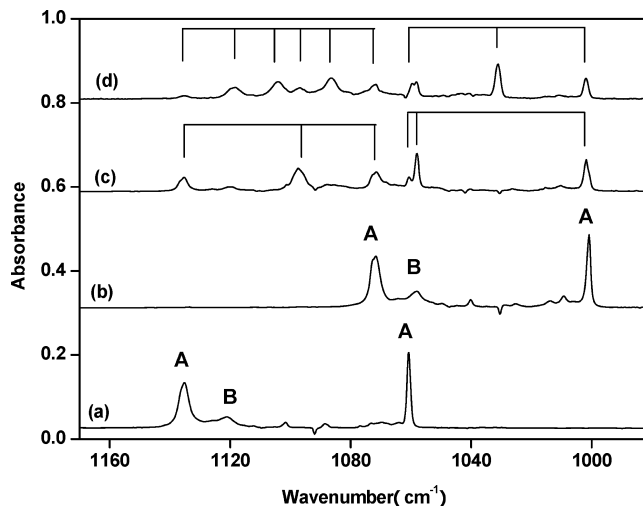


Figure 3. Difference IR spectra in the $1170\text{--}980\text{ cm}^{-1}$ region from co-deposition of laser-evaporated Cu atoms with different isotopic samples. (Spectrum taken after annealing to 35 K minus spectrum taken after 10 min of $\lambda > 850\text{ nm}$ irradiation.) (a) 0.5% $^{16}\text{O}_2$, (b) 0.5% $^{18}\text{O}_2$, (c) 0.25% $^{16}\text{O}_2 + 0.25\%$ $^{18}\text{O}_2$, and (d) 0.125% $^{16}\text{O}_2 + 0.25\%$ $^{16}\text{O}^{18}\text{O} + 0.125\%$ $^{18}\text{O}_2$.

product identification based on isotopic shifts and absorption splitting. All the infrared absorptions with O-18 substitutions are also listed in Table 1. The spectra in selected regions with different isotopic samples are shown in Figures 3 and 4, respectively.

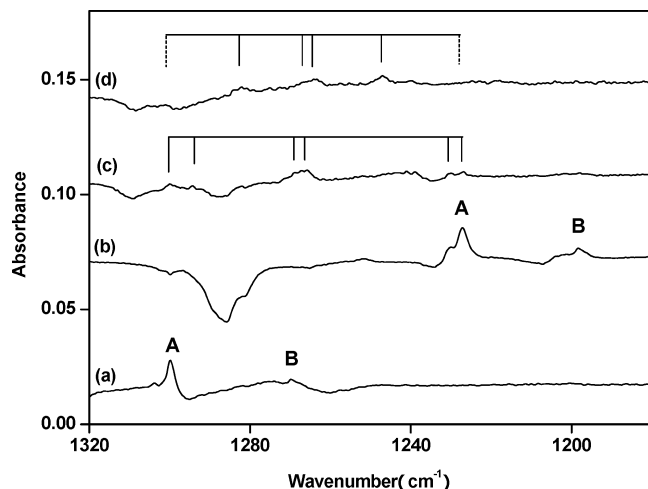
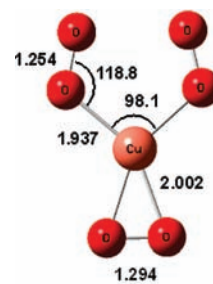


Figure 4. Difference IR spectra in the 1320–1180 cm^{-1} region from co-deposition of laser-evaporated Cu atoms with different isotopic samples. (Spectrum taken after annealing to 35 K minus spectrum taken after 10 min of $\lambda > 850$ nm irradiation.) (a) 0.5% $^{16}\text{O}_2$, (b) 0.5% $^{18}\text{O}_2$, (c) 0.25% $^{16}\text{O}_2 + 0.25\%$ $^{18}\text{O}_2$, and (d) 0.125% $^{16}\text{O}_2 + 0.25\%$ $^{16}\text{O}^{18}\text{O} + 0.125\%$ $^{18}\text{O}_2$.

The three group A absorptions at 1299.8, 1135.2, and 1060.7 cm^{-1} shifted to 1227.4, 1071.4, and 1000.9 cm^{-1} in the experiment with the $^{18}\text{O}_2$ sample. The $^{16}\text{O}/^{18}\text{O}$ isotopic frequency ratios (1.0590, 1.0595, and 1.0597) are characteristic of O–O stretching vibrations. As shown in Figures 3 and 4, trace c, the spectrum with an equal molar mixture of $^{16}\text{O}_2$ and $^{18}\text{O}_2$ revealed that the 1135.2 cm^{-1} absorption splits into a triplet with a broad intermediate absorption centered at 1097.4 cm^{-1} , while three closely spaced doublets were observed for the high-frequency mode at 1299.8 cm^{-1} . These experimental observations indicate that two equivalent O_2 subunits are involved in the absorber, and the 1299.8 cm^{-1} band is slightly coupled with another vibrational mode with the same symmetry (the low frequency O–O stretching mode of side-on bonded O_2 ligand). The infrared absorption at 1060.7 cm^{-1} shifted to 1000.9 cm^{-1} with $^{18}\text{O}_2$. The infrared spectrum from the mixed $^{16}\text{O}_2 + ^{18}\text{O}_2$ experiment revealed that three absorptions at 1060.7, 1058.1, and 1001.8 cm^{-1} were observed. The 1001.8 cm^{-1} absorption is broad and slightly blue-shifted from the pure O-18 value of 1000.9 cm^{-1} , suggesting the involvement of more than one absorption due to band overlap. An additional intermediate absorption at 1030.0 cm^{-1} was observed in the spectrum using a mixed $^{16}\text{O}_2 + ^{16}\text{O}^{18}\text{O} + ^{18}\text{O}_2$ sample (Figure 3, trace d). These isotopic spectral features indicate that the infrared absorption at 1060.7 cm^{-1} should result from a side-on bonded O_2 fragment with two equivalent O atoms, and this mode is slightly perturbed by other O_2 subunit(s). The above experimental observations indicate that the absorber of group A absorptions involves three O_2 subunits, in which two of them are equivalent while the third one is side-on bonded and should have slightly longer O–O bond length than those of the other two O_2 ligands. No other absorptions in the low-frequency region were observed to track with the group A absorptions. Accordingly, we assign the group A absorptions to a CuO_6 complex.

The group B absorptions (1269.0, 1121.6, and 1070.0 cm^{-1}) exhibit similar spectroscopic features to the above-characterized CuO_6 complex. A larger complex with a CuO_6 core loosely coordinated by one or more molecular oxygens in a solid argon matrix was proposed as the origination of group B absorptions.

The CuO_6 system has been the subject of some experimental and theoretical studies.^{26–28} Anion photoelectron spectroscopic



$\text{Cu}(\eta^2\text{-O}_2)(\eta^1\text{-O}_2)_2$ ${}^4\text{B}_1$ C_{2v}

Figure 5. Optimized structures (DFT/B3LYP) of the $\text{Cu}(\eta^2\text{-O}_2)(\eta^1\text{-O}_2)_2$ complex (bond lengths in angstrom and bond angles in degrees).

TABLE 2: Comparison Between the Observed and Calculated Vibrational Frequencies (cm^{-1}) and Infrared Intensities of the $\text{Cu}(\eta^2\text{-O}_2)(\eta^1\text{-O}_2)_2$ Complex in the ${}^4\text{B}_1$ State

mode ^a	frequency (intensity)	
	observed ^b	calculated ^c
$(\eta^1\text{-O}_2)_2$ sym. str. (a_1)	1299.8 (0.07)	1386.2 (56)
$(\eta^1\text{-O}_2)_2$ asym. str. (b_2)	1135.2 (1.00)	1230.7 (960)
$\eta^2\text{-O}_2$ str. (a_1)	1060.7 (0.59)	1210.3 (559)
$\text{Cu}(\eta^1\text{-O}_2)_2$ asym. str. (b_2)		473.1 (0)
$\text{Cu}(\eta^1\text{-O}_2)_2$ sym. str. (a_1)		452.3 (7)

^a Only the vibrations above 400 cm^{-1} are listed. ^b Integrated intensity normalized to the most intense absorption. ^c Predicted IR intensities in km/mol .

study indicates that two isomers, a copper dioxide dioxygen complex, $\text{OCuO}(\text{O}_2)_2$, and a copper dioxygen complex, $\text{Cu}(\text{O}_2)_3$, coexist in the gas phase.²⁶ However, both structures were theoretically predicted not to be the global minima on the potential energy surfaces of CuO_6 . A bisozonide structure was predicted as the ground state for the CuO_6 complex using the spin-polarized GGA method with plane-wave basis sets, but isomers containing $\text{Cu}(\text{O}_2)$ building blocks are very close in energy to that of the bisozonide structure. Among the isomers based on the $\text{Cu}(\text{O}_2)$ unit, the structure containing one side-on and two end-on bonded O_2 units with C_{2v} symmetry lies lowest in energy.²⁷ Density functional calculations using PBE functional indicate that several competitive structures exist with structures containing ozonide units, being higher in energy than those with O_2 units. The structure with one side-on and two end-on bonded O_2 units (C_{2v}) was predicted to be lowest in energy.²⁸ On the basis of our experimental observations, the experimentally observed CuO_6 species involves three O_2 units. The ozonide structures and dioxide–dioxygen structures can be ruled out. We also did calculations on CuO_6 , but focused only on the structures with a copper center coordinated by three O_2 ligands. Geometric optimizations were performed on both doublet and quartet spin states. Consistent with previous calculations,^{27,28} the D_{3h} structure is not stable, while the structure with one side-on and two end-on bonded O_2 units in C_{2v} symmetry (Figure 5) was predicted to be lowest in energy. The most stable bisozonide structure was predicted to lie about 15 kcal/mol higher in energy than the most stable C_{2v} structure at the CCSD(T)//B3LYP level of theory. It should be pointed out that DFT calculations may not be adequate enough to provide an accurate prediction of the CuO_6 species. High-level calculations are highly desired. The present calculations focused on vibrational frequencies, which can provide qualitative prediction to support the experimental assignment. As listed in Table 2, the three experimentally observed O–O stretching vibrational modes for the most stable

TABLE 3: DFT/B3LYP Calculated O–O Vibrational Frequencies (cm⁻¹) and Intensities (km/mol) of different Cu(η^2 -O₂)(η^1 -O₂)₂ Isotopomers Present in the ¹⁶O₂ + ¹⁸O₂ Experiment

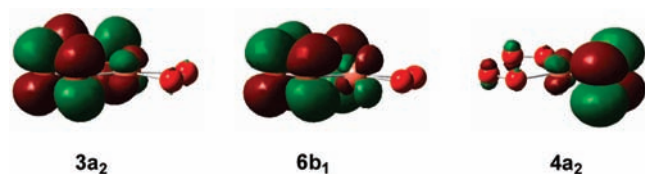
	frequency (intensity)		
	(η^1 -O ₂) ₂ (sym. str.)	(η^1 -O ₂) ₂ (asym. str.)	η^2 -O ₂ str.
Cu(η^2 - ¹⁶ O ₂)(η^1 - ¹⁶ O ₂) ₂	1386.2 (56)	1230.7 (960)	1210.3 (559)
Cu(η^2 - ¹⁸ O ₂)(η^1 - ¹⁶ O ₂) ₂	1383.8 (83)	1230.7 (960)	1143.1 (480)
Cu(η^2 - ¹⁶ O ₂)(η^1 - ¹⁶ O ₂)(η^1 - ¹⁸ O ₂)	1356.8 (93)	1184.0 (830)	1211.6 (590)
Cu(η^2 - ¹⁸ O ₂)(η^1 - ¹⁶ O ₂)(η^1 - ¹⁸ O ₂)	1353.7 (127)	1187.5 (836)	1141.6 (498)
Cu(η^2 - ¹⁶ O ₂)(η^1 - ¹⁸ O ₂) ₂	1312.3 (11)	1160.2 (853)	1205.1 (587)
Cu(η^2 - ¹⁸ O ₂)(η^1 - ¹⁸ O ₂) ₂	1306.8 (50)	1160.2 (853)	1141.1 (497)

C_{2v} structure were computed at 1386.2, 1230.7, and 1210.3 cm⁻¹ with 56:960:559 km/mol relative IR intensities, in agreement with the experimental values. Table 3 lists the predicted band positions for different isotopomers with a mechanic ¹⁶O₂ + ¹⁸O₂ mixture. The predicted isotopic splittings are in quite good agreement with the experimental observations (Table 3). Taking the symmetric stretching mode of the two end-on O₂ units as an example, this mode was predicted to split into three doublets due to weak coupling with the side-on bonded O₂ unit, just as that experimentally observed (Figure 4, trace c).

The O–O bond length for the side-on bonded O₂ fragment in CuO₆ was calculated to be 1.294 Å (Figure 5), which approaches the values of the recently characterized superoxide complexes.^{34,35} The remaining two end-on coordinated O₂ moieties possess a slightly shorter O–O distance of 1.254 Å, which is compatible with the previously reported end-on bonded copper–dioxygen complexes in the enzyme PHM.⁶ These two end-on bonded O₂ fragments can still be regarded as superoxo ligands in spite of the relatively short O–O bond length with respect to the side-on bonded superoxo ligand. Molecular orbital analysis shown in Figure 6 indicated that the three unpaired electrons are localized on the 3a₂, 6b₁, and 4a₂ molecular orbitals, which are mainly out-of-plane π^* orbitals O₂ in character. Spin-density calculations indicated that 1.47e is distributed on the side-on coordinated O₂ fragment whereas 0.65e is located on each end-on bonded O₂ ligand. Thus, the *C_{2v}* Cu(O₂)₃ complex can be formally described as a trisuperoxide Cu³⁺(O₂⁻)₃ complex. Compounds with copper in its +3 oxidation state are rare; only some copper peroxide complexes were reported to exhibit Cu(III) character.⁵

The existence of the 1:1 Cu–O₂ moiety with O₂ coordinated in either side-on or end-on fashions has been proven by a series of synthetic and spectroscopic investigations.^{3–6} The present study provides a good example in demonstrating that both side-on and end-on coordination fashions can coexist in the same monocopper center. Although mononuclear copper dioxygen complexes are unstable toward dimerization reaction to form the dinuclear copper complexes, it is facile for the mononuclear CuO₆ complex to be stabilized in a solid argon matrix without the introduction of sterically hindered ligands.

The mechanism on the formation of CuO₆ is quite interesting. Formally, one would expect that the oxygen-rich CuO₆ complex is formed via stepwise dioxygen addition reactions as that in the aluminum atom and dioxygen reactions.³⁶ The stepwise

**Figure 6.** 3D contours of the singly occupied molecular orbitals of the ⁴B₁ ground state of Cu(η^2 -O₂)(η^1 -O₂)₂ complex.

formation of Al(O₂), Al(O₂)₂, and Al(O₂)₃ is energetically favored. However, the ground state of CuO₆ was predicted to be less stable than Cu(η^2 -O₂)₂ + O₂ by 17.2 kcal/mol at the CCSD(T)//B3LYP level of theory, which can rule out ground-state Cu(η^2 -O₂)₂ complex as an intermediate in the CuO₆ formation process. The CuO₆ complex could be formed either via spontaneous coordination of two O₂ molecules to the Cu(O₂) complex or via stepwise reaction involving excited-state Cu(O₂)₂. The Cu(O₂) complex absorption was barely observed in the present experiments with relatively high O₂ concentration. Note that the CuO₆ complex is quite unstable upon infrared irradiation. As has been mentioned above, the CuO₆ absorptions transferred to the 836.0 cm⁻¹ absorption previously assigned to electronic transition of Cu(O₂)₂.⁹ This implies that the CuO₆ complex losses an end-on bonded superoxo ligand to form Cu(O₂)₂ upon IR excitation. The CuO₆ complex is calculated to be bound by 10.3 kcal/mol with respect to the Cu (²S) + 3O₂ (³ Σ_g^-) precursors at the CCSD(T)//B3LYP level, which is significantly smaller than those of other transition metal superoxide complexes such as Al(η^2 -O₂)₃ (136.1 kcal/mol) and Sc(η^2 -O₂)₃ (200.4 kcal/mol).^{36,37} The unusually low binding energy is consistent with its photosensitive behavior upon infrared irradiation.

The CuO₆ complex observed in the present experiments probably corresponds to the copper dioxygen complex structure observed in the gas-phase photoelectron spectroscopic study.²⁶ Besides the dioxygen complex structure, a copper dioxide dioxygen complex structure, OCuO(O₂)₂, was also observed in the gas-phase PES study. As has been mentioned above, all the species observed in the present experiments were formed on annealing from the ground-state copper atom and dioxygen reactions. Therefore, copper dioxide species are not expected to be formed at the present experimental conditions. The O–O bond breaking in forming copper oxide requires activation energy. However, energetic laser-ablated copper atoms are able to directly insert into dioxygen to form copper dioxide in the gas phase.¹⁵

Conclusions

The mononuclear copper dioxygen complex Cu(η^2 -O₂)(η^1 -O₂)₂ bearing both side-on and end-on bonded O₂ ligands has been prepared and characterized using matrix isolation infrared spectroscopy and theoretical calculations. The complex was generated via reaction of copper atom with dioxygen in solid argon. On the basis of quantum chemical calculations, the complex is described as a trisuperoxide species with the copper center in its unusual +3 oxidation state. The Cu(III) trisuperoxide complex losses an end-on bonded superoxo ligand in forming the Cu(O₂)₂ complex under IR irradiation.

Acknowledgment. This work was supported by the National Basic Research Program of China (2007CB815203) and National Natural Science Foundation of China (20773030 and 20703012).

References and Notes

- (1) (a) Cramer, C. J.; Tolman, W. B. *Acc. Chem. Res.* **2007**, *40*, 601. (b) Itoh, S. *Curr. Opin. Chem. Biol.* **2006**, *10*, 115. (c) Lewis, E. A.; Tolman, W. B. *Chem. Rev.* **2004**, *104*, 1047.
- (2) (a) Mirica, L. M.; Ottenwaelder, X.; Stack, T. D. P. *Chem. Rev.* **2004**, *104*, 1013. (b) Wang, L. S.; Wu, H. B.; Desai, S. R.; Lou, L. *Phys. Rev. B* **1996**, *53*, 8028.
- (3) (a) Maiti, D.; Fry, H. C.; Woertink, J. S.; Vance, M. A.; Solomon, E. I.; Karlin, K. D. *J. Am. Chem. Soc.* **2007**, *129*, 264. (b) Lanci, M. P.; Smirnov, V. V.; Cramer, C. J.; Gauchenova, E. V.; Sundermeyer, J.; Roth, J. P. *J. Am. Chem. Soc.* **2007**, *129*, 14697. (c) Sarangi, R.; Aboeella, N.; Fujisawa, K.; Tolman, W. B.; Hedman, B.; Hodgson, K. O.; Solomon, E. I. *J. Am. Chem. Soc.* **2006**, *128*, 8286. (d) Schatz, M.; Raab, V.; Foxon, S. P.; Brehm, G.; Schneider, S.; Reiher, M.; Holthausen, M. C.; Sundermeyer, J.; Schindler, S. *Angew. Chem., Int. Ed.* **2004**, *43*, 4360. (e) Smirnov, V. V.; Roth, J. P. *J. Am. Chem. Soc.* **2006**, *128*, 3683. (f) Chen, P.; Root, D. E.; Campochiaro, C.; Fujisawa, K.; Solomon, E. I. *J. Am. Chem. Soc.* **2003**, *125*, 466. (g) Weitzer, M.; Schindler, S.; Brehm, G.; Schneider, S.; Hörmann, E.; Jung, B.; Kaderli, S.; Zuberbuehler, A. D. *Inorg. Chem.* **2003**, *42*, 1800. (h) Osako, T.; Nagatomo, S.; Tachi, Y.; Kitagawa, T.; Itoh, S. *Angew. Chem., Int. Ed.* **2002**, *41*, 4325.
- (4) (a) Würtele, C.; Gaoutchenova, E.; Harms, K.; Holthausen, M. C.; Sundermeyer, J.; Schindler, S. *Angew. Chem., Int. Ed.* **2006**, *45*, 3867. (b) Aboeella, N. W.; Lewis, E. A.; Reynolds, A. M.; Brennessel, W. W.; Cramer, C. J.; Tolman, W. B. *J. Am. Chem. Soc.* **2002**, *124*, 10660. (c) Fujisawa, K.; Tanaka, M.; Moro-oko, Y.; Kitajima, N. *J. Am. Chem. Soc.* **1994**, *116*, 12079.
- (5) (a) Reynolds, A. M.; Gherman, B. F.; Cramer, C. J.; Tolman, W. B. *Inorg. Chem.* **2005**, *44*, 6989. (b) Aboeella, N. W.; Kryatov, S. V.; Gherman, B. F.; Brennessel, W. W.; Young, V. G., Jr.; Sarangi, R.; Rybak-Akimova, E. V.; Hodgson, K. O.; Hedman, B.; Solomon, E. I.; Cramer, C. J.; Tolman, W. B. *J. Am. Chem. Soc.* **2004**, *126*, 16896.
- (6) Prigge, S. T.; Eipper, B. A.; Mains, R. E.; Amzel, L. M. *Science* **2004**, *304*, 864.
- (7) Darling, J. H.; Garton-Sprenger, M. B.; Ogden, J. S. *Faraday Symp. Chem. Soc.* **1973**, *7*, 75.
- (8) (a) Tevault, D. E.; Mowery, R. L.; De Marco, R. A.; Smardzewski, R. R. *J. Chem. Phys.* **1981**, *74*, 4342. (b) Tevault, D. E. *J. Chem. Phys.* **1982**, *76*, 2859.
- (9) Ozin, G. A.; Mitchell, S. A.; García-Prieto, J. *J. Am. Chem. Soc.* **1983**, *105*, 6399.
- (10) Howard, J. A.; Sutcliffe, R.; Mile, B. *J. Phys. Chem.* **1984**, *88*, 4351.
- (11) (a) Bondybey, V. E.; English, J. H. *J. Phys. Chem.* **1984**, *88*, 2247. (b) Caspary, N.; Savchenko, E. V.; Thoma, A.; Lammers, A.; Bondybey, V. E. *Low Temp. Phys.* **2000**, *26*, 744.
- (12) Kasai, P. H.; Jones, P. M. *J. Phys. Chem.* **1986**, *90*, 4239.
- (13) Brown, C. E.; Mitchell, S. A.; Hackett, P. A. *J. Phys. Chem.* **1991**, *95*, 1062.
- (14) Wu, H. B.; Desai, S. R.; Wang, L. S. *J. Chem. Phys.* **1995**, *103*, 4363.
- (15) Chertihin, G. V.; Andrews, L.; Bauschlicher, C. W., Jr. *J. Phys. Chem. A* **1997**, *101*, 4026.
- (16) (a) Langhoff, S. R.; Bauschlicher, C. W., Jr. *Chem. Phys. Lett.* **1986**, *124*, 241. (b) Gutsev, G. L.; Andrews, L.; Bauschlicher, C. W., Jr. *Theor. Chem. Acc.* **2003**, *109*, 298. (c) Bagus, P. S.; Nelin, C. J.; Bauschlicher, C. W., Jr. *J. Chem. Phys.* **1983**, *79*, 2975. (d) Bauschlicher, C. W., Jr.; Langhoff, S. R.; Partridge, H.; Sodupe, M. *J. Phys. Chem.* **1993**, *97*, 856.
- (17) Mochizuki, Y.; Nagashima, U.; Yamamoto, S.; Kashiwagi, H. *Chem. Phys. Lett.* **1989**, *164*, 225.
- (18) Hrusak, J.; Koch, W.; Schwarz, H. *J. Chem. Phys.* **1994**, *101*, 3898.
- (19) (a) Deng, K.; Yang, J. L.; Yuan, L. F.; Zhu, Q. S. *J. Chem. Phys.* **1999**, *111*, 1477. (b) Deng, K.; Yang, J. L.; Zhu, Q. S. *J. Chem. Phys.* **2000**, *113*, 7867.
- (20) (a) Pouillon, Y.; Massobrio, C.; Celino, M. *Comput. Mater. Sci.* **2000**, *17*, 539. (b) Pouillon, Y.; Massobrio, C. *Chem. Phys. Lett.* **2000**, *331*, 290.
- (21) Gutsev, G. L.; Rao, B. K.; Jena, P. *J. Phys. Chem. A* **2000**, *104*, 11961.
- (22) Hasegawa, J.; Pierloot, K.; Roos, B. O. *Chem. Phys. Lett.* **2001**, *335*, 503.
- (23) Cao, Z. X.; Solà, M.; Xian, H.; Duran, M.; Zhang, Q. E. *Int. J. Quantum Chem.* **2001**, *81*, 162.
- (24) (a) Massobrio, C.; Pouillon, Y. *J. Chem. Phys.* **2003**, *119*, 8305. (b) Pouillon, Y.; Massobrio, C. *Appl. Surf. Sci.* **2004**, *226*, 306.
- (25) Uzunova, E. L.; Mikosch, H.; Nikolov, G. St. *J. Chem. Phys.* **2008**, *128*, 094307.
- (26) Wu, H.; Desai, S. R.; Wang, L. S. *J. Phys. Chem. A* **1997**, *101*, 2103.
- (27) Pouillon, Y.; Massobrio, C. *Chem. Phys. Lett.* **2002**, *356*, 469.
- (28) Baruah, T.; Zope, R. R.; Pederson, M. P. *Phys. Rev. A* **2004**, *69*, 023201.
- (29) (a) Wang, G. J.; Zhou, M. F. *Int. Rev. Phys. Chem.* **2008**, *27*, 1. (b) Zhou, M. F.; Andrews, L.; Bauschlicher, C. W., Jr. *Chem. Rev.* **2001**, *101*, 1931.
- (30) Frisch, M. J.; Trucks, G. W.; Schlegel, H. B.; Scuseria, G. E.; Robb, M. A.; Cheeseman, J. R.; Montgomery, J. A., Jr.; Vreven, T.; Kudin, K. N.; Burant, J. C.; Millam, J. M.; Iyengar, S. S.; Tomasi, J.; Barone, V.; Mennucci, B.; Cossi, M.; Scalmani, G.; Rega, N.; Petersson, G. A.; Nakatsuji, H.; Hada, M.; Ehara, M.; Toyota, K.; Fukuda, R.; Hasegawa, J.; Ishida, M.; Nakajima, T.; Honda, Y.; Kitao, O.; Nakai, H.; Klene, M.; Li, X.; Knox, J. E.; Hratchian, H. P.; Cross, J. B.; Adamo, C.; Jaramillo, J.; Gomperts, R.; Stratmann, R. E.; Yazyev, O.; Austin, A. J.; Cammi, R.; Clifford, S.; Cioslowski, J.; Stefanov, B. B.; Liu, G.; Liashenko, A.; Piskorz, P.; Komaromi, I.; Martin, R. L.; Fox, D. J.; Keith, T.; Al-Laham, M. A.; Peng, C. Y.; Nanayakkara, A.; Challacombe, M.; Gill, P. M. W.; Johnson, B.; Chen, W.; Wong, M. W.; Gonzalez, C.; Pople, J. A. *Gaussian 03, Revision B.05*; Gaussian, Inc.: Pittsburgh, PA, 2003.
- (31) (a) Becke, A. D. *J. Chem. Phys.* **1993**, *98*, 5648. (b) Lee, C.; Yang, W.; Parr, R. G. *Phys. Rev. B* **1988**, *37*, 785.
- (32) (a) McLean, A. D.; Chandler, G. S. *J. Chem. Phys.* **1980**, *72*, 5639. (b) Krishnan, R.; Binkley, J. S.; Seeger, R.; Pople, J. A. *J. Chem. Phys.* **1980**, *72*, 650.
- (33) Chertihin, G. V.; Andrews, L. *J. Chem. Phys.* **1998**, *108*, 6404.
- (34) (a) Cramer, C. J.; Tolman, W. B.; Theopold, K. H.; Rheingold, A. L. *Proc. Natl. Acad. Sci. U.S.A.* **2003**, *100*, 3635. (b) Bahlo, J.; Himmel, H. J.; Schnöckel, H. *Angew. Chem., Int. Ed.* **2001**, *40*, 4696.
- (35) (a) Gong, Y.; Zhou, M. F. *J. Phys. Chem. A* **2008**, *112*, 9758. (b) Gong, Y.; Wang, G. J.; Zhou, M. F. *J. Phys. Chem. A* **2008**, *112*, 4936. (c) Zhao, Y. Y.; Zheng, X. M.; Zhou, M. F. *Chem. Phys.* **2008**, *351*, 13. (d) Zhao, Y. Y.; Su, J.; Gong, Y.; Li, J.; Zhou, M. F. *J. Phys. Chem. A* **2008**, *112*, 8606. (e) Gong, Y.; Zhou, M. F.; Tian, S. X.; Yang, J. L. *J. Phys. Chem. A* **2007**, *111*, 6127. (f) Gong, Y.; Zhou, M. F. *J. Phys. Chem. A* **2007**, *111*, 8973. (g) Yang, R.; Gong, Y.; Zhou, M. F. *Chem. Phys.* **2007**, *340*, 134.
- (36) Stöbber, G.; Schnöckel, H. *Angew. Chem., Int. Ed.* **2005**, *44*, 4261.
- (37) Gong, Y.; Ding, C. F.; Zhou, M. F. *J. Phys. Chem. A* **2007**, *111*, 11572.